BNL-224464-2023-TECH
EIC-ADD-TN-059

ESR Dipole Power Supply Current Ripple and Noise Specifications

B. Podobedov

May 2023

Electron-Ion Collider
Brookhaven National Laboratory

U.S. Department of Energy
USDOE Office of Science (SC), Nuclear Physics (NP) (SC-26)

DISCLAIMER

ESR Dipole Power Supply Current Ripple and Noise Specifications

Boris Podobedov, Michael Blaskiewicz, Yun Luo, Daniel Marx, Christoph Montag, Derong Xu, Brookhaven National Laboratory, Upton, NY, 11733, USA

(Dated: May 23, 2023)

I. INTRODUCTION

This note presents key findings for the ESR main magnet dipole power supplies (PS), where we find the current ripple specification to be close to or beyond the state-of-the-art. These specifications originate from beam-beam considerations, with the requirement to limit the ripple-induced hadron emittance growth to below 10%/hour.

Beam dynamics that drive this PS ripple specification arise from the beam motions at the Interaction Point (IP). The frequency of the motions can be separated into "low", compared to the betatron frequency, and "high", i.e. around the betatron frequency and harmonics. In terms of the driving frequency, "low" implies $f << f_0\,\nu_{x,y}$ and "fast" means $f \approx \{f_0\,\nu_{x,y}$, $f_0\,(1-\nu_{x,y})$, etc.$\}$, where $f_0 = 1/T_0$=78.2 kHz is the revolution frequency, and $\nu_{x,y}$ are the fractional parts of the betatron tunes. Frequencies higher than $f_0/2$ will be folded back due to the particles sampling the field once per turn.

To provide flexibility for future lattice adjustments and working point variations, we do not consider the tunes as fixed. Instead, we assume a certain margin and allow them to potentially fall within the range of $0.1 < \nu_{x,y} < 0.5$. In other words, the high-frequency region spans approximately from 8 kHz to 40 kHz. Consequently, we define the dipole PS ripple in two distinct frequency ranges: the low-frequency range of [1-8000] Hz and the high-frequency range of [8-40] kHz.

For the physics effects we analyzed in this note, there is no distinction between the ripple (which can be approximately reproduced in the frequency domain) and random noise if both have some power within the frequency bandwidth of interest. Therefore, while we will use the term "ripple" for short, it should always be understood that we are referring to "ripple plus noise".

Except for the lower end of the low-frequency range, the impact of the rippling PS current on the beam will be considerably reduced due to the eddy currents induced in the walls of the vacuum chamber. We will account for this effect in the PS ripple specifications to follow.

The remaining sections of this note are structured as follows: Section II outlines the beam-beam physics requirements for the positional stability of the beam at the IP. Section III describes the anticipated shielding effect of the eddy currents induced in the vacuum chamber. Section IV derives the ripple requirement for the low-frequency range by propagating the closed orbit ripple resulting from the rippling dipoles to the IP (relevant lattice

simulation results are summarized in the Appendix). In Section V, we present the analytical criterion for the ripple in the high-frequency range by considering resonant oscillations of the electron beam around a stable closed orbit near the betatron frequency. Finally, Section VI provides a summary of our findings and discusses related work.

II. BEAM-BEAM REQUIREMENTS FOR RELATIVE POSITIONAL STABILITY OF COLLIDING BEAMS

The luminosity reduction due to imperfect transverse beam overlap at the IP can be estimated by the factor $e^{-\frac{1}{4}(\delta_x^2+\delta_y^2)}$, where $\delta_{x,y}$ are the distances between the colliding beam centers in each plane in units of the corresponding rms beam size. For instance, assuming equal δ_x and δ_y and allowing no more than 5% luminosity reduction requires the relative orbit jitter at the IP to be below 32% of the corresponding rms size.

A much more stringent requirement for beam positional stability at the IP comes from dynamical aspects of beam-beam interaction, specifically the beam-beam kick modulation leading to the emittance growth of the hadron beam. For instance, as was shown analytically [1] as well as by means of weak-strong beam-beam simulations [2], to keep the emittance growth within 10% per hour, the amplitude of electron beam centroid oscillations at the proton betatron frequency needs to be limited to about 10^{-4} fraction of the rms beam size.

Even at much lower frequencies, the positional stability at the IP must be maintained at a percent level of the rms beam size in each plane. This is illustrated in Fig. 1 which shows the proton beam size evolution when the electron beam centroid is oscillating near 60 Hz. Unacceptably high emittance growth occurs at higher oscillation amplitudes. Importantly, while the growth mainly occurs in the vertical plane, it is driven both by the horizontal and vertical orbit ripple. Even the cases of purely horizontal ripple result in the vertical growth via beam-beam-induced betatron and synchro-betatron coupling.

Fig. 1, as well as the more detailed analysis [2], suggest that to keep the vertical emittance growth within 10% per hour, the motion at the IP must be maintained within 1% of the beam size in both planes. (Alternative configurations with somewhat higher noise in one plane at the expense of the other could also be acceptable.) This conclusion, as well as Fig. 1, apply to the simulations performed at the reference proton beam tunes. Further studies in [2] showed that proton tune optimization allows one to relax the requirement for

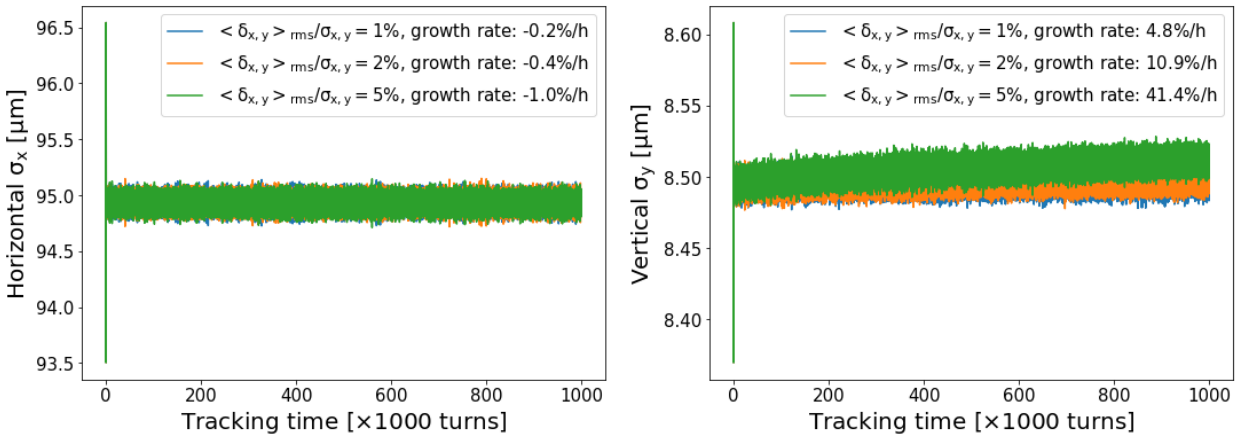

FIG. 1. Proton beam size evolution from weak-strong simulation when the electron beam is undergoing positional oscillations amounting to 1, 2, or 5% of the rms beam size in each plane. The oscillations are band-limited to [55-65] Hz range, with uniform magnitude and random phase. Fitted beam size growth rates are shown in the legend.

the motions at the IP to 2.5% of the beam size. In this note, we take the last number to establish the ESR PS ripple tolerance at low frequencies, i.e. we require that at the IP, $\langle \Delta x \rangle_{\rm rms}/\sigma_x \leq 0.025$.

Another conclusion of beam-beam studies for low perturbation frequencies is that the proton emittance growth is independent of the orbit ripple bandwidth. What matters is the total rms orbit ripple in the time domain, $\langle \Delta x \rangle_{\rm rms}$, or, equivalently, the square root of the orbit ripple power spectral density[1], $P_{\Delta x}(f)$, integrated over all frequencies, $\left(\int_{1\ Hz}^{8\ kHz} df P_{\Delta x}(f) \right)^{1/2}$.

In contrast, at high frequencies, we mainly want to restrict the electron beam oscillation near the proton betatron frequency, which is fixed for a given working point. If a ripple line, or some broad-band noise component, hits this frequency line (which is assumed to have a bandwidth of ±400 Hz corresponding to the tune spread of ±0.005, explained in Section V), the other potential ripple lines, spread by more than 800 Hz apart, will miss it. Therefore, at the high-frequency range, the PS current ripple specifications will be set for the maximum amplitude of the PS current power spectral density $P_{\delta I}(f)$, i.e. no frequency integration is needed.

In addition to the beam centroid stability at the IP, beam-beam considerations impose

[1] We use one-sided power spectral density (PSD) so that for continuous signal $x(t)$ the average power is $\mathrm{var}(x) = \int_0^\infty df P_x(f)$. For discrete signals, the PSD contains the total power of the signal in the frequency interval from DC to half of the Nyquist rate.

limits for the maximum allowable electron beam size variation. These limits also depend on the frequency of the variation, with frequencies near twice the hadron betatron tunes being the most dangerous. However, these limits, presently at a few percent of beam size at each plane, are not very restrictive and so they do not define any PS specifications. Instead, the quadrupole PS ripple specifications largely follow from the required tune stability, i.e. something not directly related to beam-beam interaction.

We emphasize that all beam-beam simulations to-date were performed at 10 GeV electron beam energy. The PS ripple specifications to be derived in this note assume that similar levels of beam stability at the IP will be required at all operational energies of the ESR.

III. EDDY CURRENT SHIELDING

At high frequencies, the oscillations of the beam caused by the current ripple in the magnet PS are significantly attenuated by the eddy currents in the vacuum chamber walls and in the magnets themselves. To maintain a conservative approach while ensuring simplicity, we focus our estimation on the attenuation due to the chamber, which is then accounted for in the ripple specifications.

Apart from minor details related to the cooling channels and ante-chamber (the latter has been removed in the latest design), the copper vacuum chamber at the dipoles [see [3] Fig. 6.125] can be described as an ellipse with a wall thickness of $d = 4$ mm and inner semi-axes measuring 40 mm and 18 mm. For the purpose of this analysis, we conservatively approximated the chambers with a circular cross-section having an inner radius of $b = 18$ mm. The conductivity value σ_c=$5.8\times10^7(\Omega \times m)^{-1}$ was used for copper.

The electromagnetic shielding was determined by employing an exact analytical expression for the transfer function, which accommodates arbitrary ratios of wall thickness to skin depth. The specific formulation of this expression, involving modified Bessel functions, is not presented here (refer to [4] for the derivation and underlying assumptions). Instead, in Fig. 2, we plot the resulting attenuation factor. This factor represents the magnitude of the transfer function for the AC-varying dipole field inside the chamber relative to that outside of it. Additionally, we provide a useful approximation proposed in [5], which offers a concise representation of the transfer function using N lowest frequency poles,

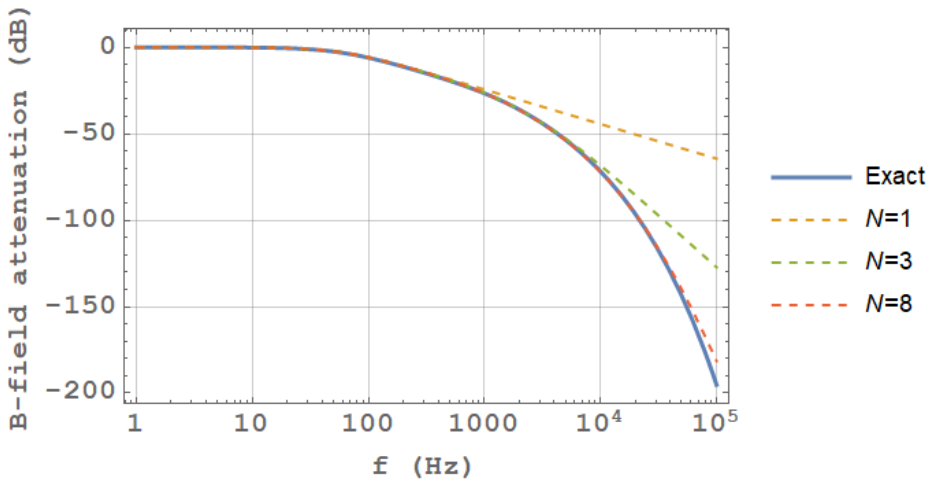

FIG. 2. Dipole field ripple attenuation for Cu chamber with a circular cross-section of 18 mm inner radius and 4 mm wall thickness together with N=1-, 3-, and 8-pole approximations from Eq. (1).

$$\tilde{T}(p) = \frac{\tilde{B}(p)_{\text{int}}}{\tilde{B}(p)_{\text{ext}}} \approx \prod_{n=0}^{N-1} \frac{p_n}{(p+p_n)}, \tag{1}$$

where p is the Laplace variable and the poles are given by

$$p_0 = -\left(\mu_0 \sigma_c \, b \, d/2\right)^{-1}, \tag{2}$$

$$p_{n>0} = -n^2 \frac{\pi^2}{\mu_0 \sigma_c d^2}, \tag{3}$$

with μ_0 denoting the permeability of free space.

For the circular approximation of the ESR chamber, $|p_0|/2\pi$=60.66 Hz[2] and $|p_{n>0}|/2\pi = n^2 \times 1347$ Hz. Several dominant pole approximations are plotted in Fig. 2. Evidently, N=3 poles give a very accurate approximation up to 8 kHz, while the N=8 approximation is accurate to within 2 dB up to 40 kHz.

It is worth mentioning that the $n > 0$ poles given by Eq. (3) correspond to frequencies where the skin depth is equal to $\frac{\sqrt{2}}{\pi} \, d/n$. To accurately describe the ESR chamber transfer function at frequencies where the skin depth is comparable or smaller than the wall thickness, multiple of these poles are required. For example, at 10 kHz, the skin depth is 0.66 mm and much smaller than the wall thickness.

Clearly, the attenuation provided by the eddy currents is significant, except at the lower

[2] A more accurate approximation [5] which accounts for the chamber ellipticity lowers this to 29.52 Hz

end of the low frequency range. For instance, the attenuation at a few selected power-line harmonics is approximately 3 dB (60 Hz), 10 dB (180 Hz), and 23 dB (720 Hz).

IV. POWER SUPPLY RIPPLE AT FREQUENCIES 1-8000 HZ

In this frequency region, the two primary causes of the electron beam orbit jitter at the IP are the dipole magnet PS ripple and the quadrupole magnet vibrations (treated in [6]). Closed orbit perturbation due to rippling dipoles can be described analytically. In the simplest case of a large number of dipoles, $N_d >> 1$, with an uncorrelated ripple of the fractional strength $\delta\theta/\theta$, the rms orbit ripple at the IP is given by (index "x" omitted)

$$\left\langle \Delta x \right\rangle_{\rm rms} = \frac{\pi\sqrt{\bar{\beta}\ \beta^*}}{\sqrt{2N_d}\,|\sin(\pi\nu)|}\delta\theta/\theta, \tag{4}$$

where $\bar{\beta}$ is the average beta function, θ is the nominal bend angle, $\delta\theta =< \theta >_{\rm rms}$. Estimating this for the typical ESR lattice parameters (e.g. $\bar{\beta}$=30 m, β^*=0.4 m, $N_d = 670$, $\nu = 0.12$) results in about one-micron rms per $\delta\theta/\theta = 10^{-6}$ fractional ripple. This suggests that to passively maintain the orbit to within 1% of $\sigma \approx 100$ μm horizontal beam size, the dipole PS current ripple $\delta I/I \approx \delta B/B = \delta\theta/\theta$ on the order of one part-per-million (ppm) would be required. Note that here the PS ripple is assumed normalized to the operating current value.

More accurately, the orbit ripple for a given amount of dipole field ripple can be calculated with lattice codes. Simulations of the IP orbit ripple for a large number of dipole field error sets were performed in Elegant [7] and MAD-X [8] for v.5.6 1- and 2-IP lattices at 6, 10, and 18 GeV. Cases of uncorrelated magnet errors, as well as the ones with equal errors for the magnets sharing a common dipole PS, were simulated. For the fractional field strength error of 10^{-4} and the lattice tunes $\nu_x = 0.12, \nu_y = 0.1$, the values of IP orbit ripple were found to be in the range from about 30 to 200 microns (see Appendix for more detail). This is generally in good agreement with Eq. (4) or similar expressions which account for the magnet families. Conservatively assuming that the horizontal tune could end up as low as 0.1, for the final specifications the results were scaled by $\sin(\pi\ 0.12)/\sin(\pi\ 0.1) \approx 1.19$.

The final ripple specifications need to be normalized to the maximum PS current, $I_{\rm max}$. With the exception of short arc bends, the dipole bend angles remain constant across all operating energies, while their maximum PS currents scale proportionally to the energy.

Therefore, the lattice with the largest ratio of the simulated IP jitter to the beam energy (6 GeV 2-IP) was taken to define the ripple specifications. Requiring the IP orbit jitter to be at 2.5% of the rms beam size resulted in 0.5 ppm current ripple normalized to the values from 18 GeV operation. The short arc bend supply ends up with a more relaxed, 1.5 ppm specification.

So far we did not take credit for the eddy current shielding. This could be done by performing the frequency integration weighted with the attenuation factor from Fig. 2. The resulting specifications restrict the power spectral density of the PS current ripple $P_{\delta I}(f)$ by

$$\sqrt{\int_{1\ \mathrm{Hz}}^{8\ \mathrm{kHz}} df\ P_{\delta I}(f)\ |\tilde{T}(i2\pi f)|^2} \leq \begin{cases} 0.5\times 10^{-6}\ I_{\max} & \text{(most dipoles)} \\ 1.5\times 10^{-6}\ I_{\max} & \text{(short arc bends)} \end{cases}, \tag{5}$$

with the function $\tilde{T}(...)$ defined by Eq. (1), where the product truncation at N=3 terms provides sufficient accuracy.

V. POWER SUPPLY RIPPLE AT FREQUENCIES 8-40 KHZ

In this frequency range, the beam motion can be resonantly excited close to the betatron frequency. Apart from the excitation potentially coming from the dipole PS it could be caused by the main [9] and crab-cavity [10] RF system noise, as well as by some collective instabilities (e.g. [1]). The analytical derivation that propagates the rippling dipole field to the beam motion at the IP is presented elsewhere [11]. Here we give a brief summary.

A dipole kick, located at $s = 0$, oscillating at the betatron frequency as $\hat{\theta}_0 \sin(\omega_\beta t + \phi)$ would cause resonant oscillations of the beam centroid around the closed orbit with the amplitude

$$\hat{x}(s) = \frac{\hat{\theta}_0 \sqrt{\beta(0)\beta(s)}}{2\alpha T_0}, \tag{6}$$

where $\hat{\theta}_0$ is the kick amplitude and $(\alpha T_0)^{-1} \gg 1$ is the damping time in turns.

The effect of multiple kicks $\hat{\theta}_{0,i}$, located at s_i, can be found by summation, which must also account for the betatron phases $\psi(s_i)$, as well as for the oscillation phases ϕ_i and other factors, which are impossible to accurately estimate for the ESR magnets at this time. The most conservative estimate is therefore to assume that the oscillating kicks from all rippling dipoles add in phase. Then, for the required $x_{\mathrm{rms}} = 10^{-4}\sigma$ at the IP, the field ripple can be

estimated as

$$\left\langle \delta B/B \right\rangle_{\rm rms} = 10^{-4}\sigma \frac{\alpha T_0}{\pi\sqrt{\bar{\beta}\beta^*}}. \tag{7}$$

Taking 100-turn damping (with beam-beam) results in $\left\langle \delta B/B \right\rangle_{\rm rms} \approx 9.2\times 10^{-12}$. A numerically equivalent estimate in terms of the field power spectral density at the tune frequency was also obtained for the case of white-noise variation of the field [11].

Even this very conservative estimate implies that, for instance, a 1 ppm dipole PS current ripple at the tune frequency would be acceptable, as long as 5 orders of magnitude of additional attenuation is coming from elsewhere. As is clear from Fig. 2, the vacuum chamber shielding results in this amount of attenuation at frequencies exceeding 22 kHz. The switching frequencies for the ESR magnet PS are expected to be higher, so the high-frequency ripple requirement is not too restrictive.

In reality, the dipole ripples will not add in phase, and at least $N_d^{-1/2}$ additional cancellation can be safely assumed. With this assumption, and taking the full width of the tune line to be on the order of 1/10th of the maximum beam-beam parameter, $\Delta\nu$=0.01, the maximum power spectral density of the field ripple becomes

$$P_{\delta B/B} = \frac{T_0}{\Delta\nu}\left(10^{-4}\sigma\sqrt{N_d}\frac{\alpha T_0}{\pi\sqrt{\bar{\beta}\beta^*}}\right)^2. \tag{8}$$

Dividing this expression by the attenuation factor shown in Fig. 2, and (except for the short arc bends) accounting for the 5/18 factor for the ESR energy variation we finally get the maximum allowable power spectral density for the dipole PS current ripple, $P_{\delta I/I_{\rm max}}$, plotted in Fig. 3. For the short arc bends the specification can be relaxed by a factor of three.

For narrow-band or purely harmonic ripple lines this specification should be applied after frequency smoothing over ±400 Hz bandwidth which corresponds to ±0.005 in tune. An equivalent specification follows directly from the numerical estimate right after Eq. (7),

$$\frac{\left\langle \delta I(f) \right\rangle_{\rm rms}}{I_{\rm max}} \le 9.2\times 10^{-12}\,\frac{5}{18}\frac{\sqrt{N_d}}{|\tilde{T}(i2\pi f)|} = 6.6\times 10^{-11}\frac{1}{|\tilde{T}(i2\pi f)|}, \tag{9}$$

where $\tilde{T}(...)$ is defined in Eq. (1) for which the product truncation at N=8 terms provides sufficient accuracy.

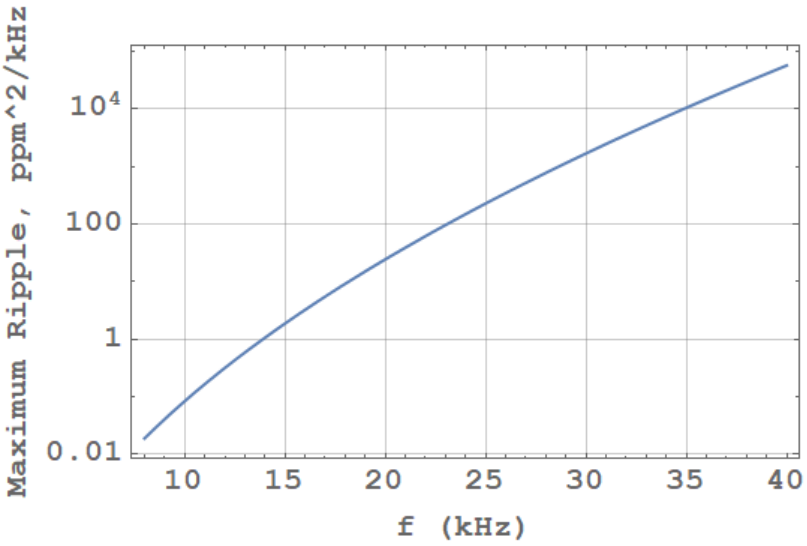

FIG. 3. Maximum dipole PS rms current ripple normalized to 18 GeV operational current. This requirement applies only in the frequency range shown, corresponding to the tune range of [0.1-0.5].

VI. SUMMARY AND DISCUSSION

The rms current ripple (plus noise) for the majority of the ESR dipole magnet power supplies, integrated over the [1-8000] Hz range and normalized to the maximum operating current, must be at or below 0.5 ppm. Using Eq. (5), the integration can account for eddy current shielding which provides significant ripple attenuation across most of this frequency range (see Fig. 2).

For the short arc bend supplies, the corresponding specification is 1.5 ppm.

In the high-frequency range of [8-40] kHz, the power spectral density of the PS current ripple (plus noise) must be below the curve depicted in Fig. 3, which already incorporates eddy current shielding. For purely harmonic lines, this specification should be applied after frequency smoothing over a bandwidth of ± 400 Hz, or the equivalent specification from Eq. (9) can be used instead. In the case of the short arc bend supplies, the high-frequency range ripple (plus noise) specification is relaxed by a factor of three compared to the rest of the dipole magnet supplies.

If the switching frequency of the power supplies exceeds 20 kHz, the high-frequency ripple specification does not appear to be overly restrictive. However, the low-frequency specifications at 0.5 and 1.5 ppm are near or beyond the state-of-the-art. For reference, the dipole PS ripple specifications for the HL-LHC [12] and SuperKEKB [13] are 1 ppm rms.

The yet-to-be-designed IP orbit feedback system should significantly reduce the orbit ripple, especially at lower frequencies, potentially relaxing the power supply ripple specifications. However, at this stage of the design, we conservatively specify the power supply ripple without considering any orbit feedback system. We will revisit this aspect in the future, if necessary.

We emphasize that the specifications derived in this note are based on the beam-beam simulations performed at 10 GeV electron beam energy. These specifications will be updated should future studies of beam-beam dynamics at 5 GeV result in substantially different sensitivity to the beam motion at the IP.

---

[1] M. Blaskiewicz, NAPAC'2019, TUPLM11

[2] D. Xu, M. Blaskiewicz, Y. Luo, D. Marx, C. Montag, B. Podobedov, IPAC'2023, MOPA039

[3] F. Willeke, F, and J. Beebe-Wang, Electron Ion Collider Conceptual Design Report 2021. doi:10.2172/1765663

[4] B. Podobedov, M. Blaskiewicz, Eddy current shielding of the magnetic field ripple in the EIC Electron Storage Ring vacuum chambers, EIC-ADD-TN-055, TBC

[5] B. Podobedov L. Ecker, D. Harder, G. Rakowsky, PAC'09, TH5PFP083

[6] B. Podobedov, D. Marx, BNL-222179-2021-TECH

[7] M. Borland, "elegant: A Flexible SDDS-Compliant Code for Accelerator Simulation," Advanced Photon Source LS-287, September 2000

[8] MAD-X, http://mad.web.cern.ch

[9] B. Podobedov, M. Blaskiewicz, BNL-215885-2020-TECH

[10] P. Baudrenghien, T. Mastoridis, Phys. Rev. Accel. Beam, 18, 101001 (2015)

[11] B. Podobedov, M. Blaskiewicz, Transversely Driven Coherent Beam Oscillations in the EIC Electron Storage Ring, EIC-ADD-TN-054, TBC

[12] High-Luminosity Large Hadron Collider (HL-LHC) Preliminary Design Report (2014)

[13] SuperKEKB Technical Design Report (2020)

Appendix A: Orbit ripple simulations

Simulations of the IP closed orbit ripple for a large number of dipole field error sets were performed in Elegant and MAD-X for v.5.6 1- and 2-IP lattices at 6, 10, and 18 GeV. The lattice tunes were set to $\nu_x = 0.12, \nu_y = 0.1$. Cases of uncorrelated magnet errors, as well as the ones with equal errors for the dipole magnets sharing a common PS, were simulated. For the latter case we used three strings: long arc dipoles (D01[AB]_), short arc dipoles (D23_), and spin rotator / IR dipoles (DB23_). Our results for the orbit ripple at the IP at the fractional dipole field strength error of $(\delta B/B)_{\rm rms} = 10^{-4}$=100 ppm are listed in the table below. We also confirmed that at this and lower field strength error levels, the rms orbit ripple scales proportionally to the rms field strength error.

Lattice v. 5.6 configuraton	x-orbit rms (microns), uncorrelated dipoles	x-orbit rms (microns), dipole strings
6 GeV/100 GeV, 1 IP	178	46.6
6 GeV/100 GeV, 2 IP	193	141
10 GeV/275 GeV, 1 IP	80.6	30.7
10 GeV/275 GeV, 2 IP	132	192
18 GeV, 1 IP	88.8	50.4
18 GeV, 2 IP	100	63.5

TABLE I. Orbit ripple at the IP for the dipole magnet fractional rms strength error of 10^{-4}.